объединенный
институт
ядерных
исследований
дубна

E9-93-401

E.L.Saldin*, E.A.Schneidmiller*, M.V.Yurkov

HIGH-EFFICIENCY FEL OSCILLATOR WITH TIME-DEPENDENT MICROWAVE FIELD IN INTERACTION REGION

Submitted to «Optics Communications»

---

*Automatic Systems Corporation, Smyshlyaevskoe Shosse 1a, 443050 Samara, Russia

1993

1 Introduction

Nowadays, when free electron lasers have come a long way from the first experimental demonstration [1] to their wide applications in various regions of science and industry, the problem to increase an efficiency of FEL devices becomes a central one for free electron laser physics and technique.

The efficiency of a FEL amplifier with homogeneous undulator is of an order of the ratio of the undulator period λ_w to the gain length l_g, and for the FEL amplifiers of infrared and visible wavelength ranges it is of an order of percent. A reliable method to increase the FEL amplifier efficiency was proposed more than ten years ago [2, 3]. The main idea of this approach is to sustain the synchronism of the electrons with amplified electromagnetic wave by means of undulator tapering. At first this idea has been confirmed by the results of numerical simulations [4, 5] and later it has been demonstrated experimentally, an efficiency $\eta \simeq 34\%$ was achieved [6]. As a result, now there exists a good consent among the physical community that the method to increase the FEL amplifier efficiency by the undulator tapering is the most optimal one.

On the other hand, the problem to increase a FEL oscillator efficiency has appeared to be more complicated. First, the efficiency of the FEL oscillator with a homogeneous undulator is rather small, $\eta \simeq 0.29/N$, where N is the number of the undulator periods [7, 8]. Usually N is about several tens which results in the FEL efficiency η less than one percent. Second, undulator tapering does not give such excellent results with respect to the FEL amplifier, it enables one to increase the FEL oscillator efficiency by a factor of 2 or 3. Using additional possibilities, such as a prebuncher, one increases the efficiency additionally by a factor of two [9]. In any case the maximal FEL oscillator efficiency does not exceed a value of several percent.

Such a significant difference in the efficiency between the FEL amplifier and FEL oscillator configurations was analyzed in detail in ref. [10]. It was shown that there is principal difference between these two FEL configurations when undulator tapering is used. In the case of the FEL amplifier, the frequency of the amplified wave is determined by a master oscillator, the initial conditions at the undulator entrance are fixed, the process of the field amplification develops in space, and, as a result, spatial tapering of the undulator parameters enables one to trap a significant fraction of the electrons in the regime of coherent deceleration. Contrary to this, the lasing frequency of the FEL oscillator depends on the value of the undulator tapering depth and is defined by the condition of the maximum of the small-signal gain in the linear mode of operation. Another difference is that the initial conditions at the undulator entrance depend on time due to the dependence on time of the field stored in the resonator. As a result, the dependence of the FEL oscillator efficiency on the tapering depth is nonmonotonous and breaking and the final FEL oscillator efficiency does not increase significantly with respect to the case of homogeneous undulator [10].

So, it seems impossible to achieve a high efficiency in the FEL oscillator using the conventional approach of undulator tapering. On the other hand, one should remember the history of the acceleration technique development. In the mid–1940s it was an idea by McMillan and Veksler to use the principle of phase stability of the particle motion in time-dependent electromagnetic fields, which has led to the invention of synchrotron and opened a way to reach superhigh energies [11, 12]. It is evident now that only an approach similar to that proposed by McMillan and Veksler may solve the problem to construct the high-efficiency FEL oscillators. For the first time such an approach to increase the FEL oscillator efficiency was proposed in ref. [13]. It is based on a natural feature of the FEL oscillator, namely the dependence on time of the radiation field stored in the resonator. It was proposed to introduce time-dependent accelerating fields into the interaction region (which is equivalent in its action to the undulator tapering). As a result, this makes it possible to trap electrons into the ponderomotive well and perform conversion of the microwave energy to the optical one. To increase number of trapped electrons (which results in higher efficiency), the authors of ref. [13] proposed to use a prebuncher together with a homogeneous undulator. Numerical estimations, presented in refs. [13, 14] have shown that an efficiency of about several tens percent can be achieved in such modification of the FEL oscillator.

There is another way to realize the idea of time-dependent variation of the FEL oscillator parameters to increase the efficiency. It was proposed to change in time the magnetic field of the undulator rather than to introduce the accelerating field into the interaction region [15, 16]. The feasibility of this method has been confirmed by the results of numerical simulations. It was shown that the high efficiency ($\eta \sim 20\%$) FEL oscillator operating in the continuous or quasi-continuous mode may be constructed at the present level of accelerator technique R&D [16].

The present paper is devoted to the problem of increase in the FEL oscillator efficiency by application of time-dependent microwave fields. Here we make an attempt to develop ideas presented in refs. [13, 14] where some novel FEL schemes have been proposed. In our opinion, giving a possibility to increase significantly the FEL oscillator efficiency, they are rather comprehensive and require significant development of novel undulator and RF structure technology. In the present paper we propose several alternative technical solutions totally based on a well developed conventional RF structure and undulator technology.

The paper proceeds as follows. In section 2 we perform a qualitative analysis of

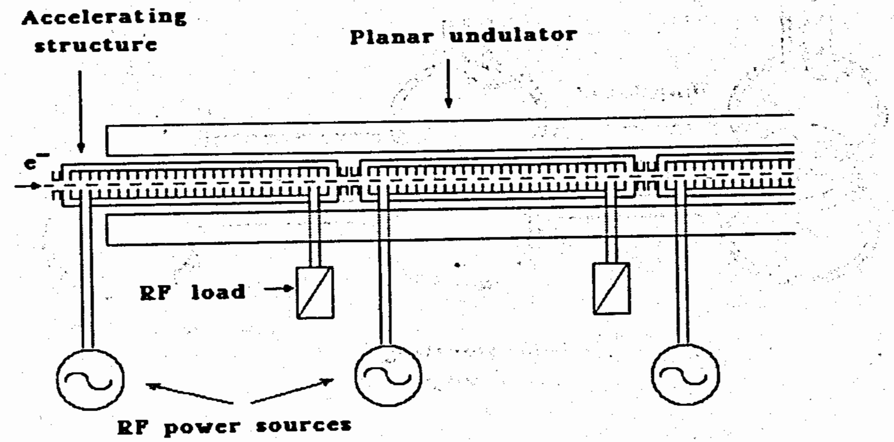

Figure 1: Scheme A: Accelerating structure combined with the main undulator

the proposed FEL schemes and obtain simple physical formulae for maximal attainable efficiency. Then, in sections 3 – 5 we perform a more detailed study using results of numerical simulations in the framework of one-dimensional FEL model. The analysis performed takes into account such effects as energy spread of electrons in the beam, dependence of the electron oscillation angle on the electron energy, change of the optical field amplitude and RF field amplitude along the undulator axis, etc.

A common feature of three proposed schemes A, B and C is that their magnetic systems consist of a prebuncher and the main undulator spaced by the drift (or dispersion) section and time-dependent RF fields are introduced inside the location of the main undulator.

Scheme A, considered in section 3, is close to that considered in papers [13, 14]. The only difference is that we propose another way for technical realization of this scheme. We propose to use the conventional undulator and RF technology by placing inside the gap of the undulator (for instance, a permanent magnet one) of an iris-loaded waveguide (one or more sections) which is fed by a RF power supply operating at a harmonic frequency of the driving accelerator (see Fig.1). A choice of a RF band is defined by the following technical limitations. First, to minimize a value of the undulator gap, one should minimize transverse dimensions of the waveguide by choosing as short RF wavelength as possible. On the other hand, there should exist well developed RF amplifiers providing the necessary RF power level to achieve the required accelerating rate. Analysis of the present-day situation with RF sources shows that the most appropriate RF band for this purpose is the X-band one.

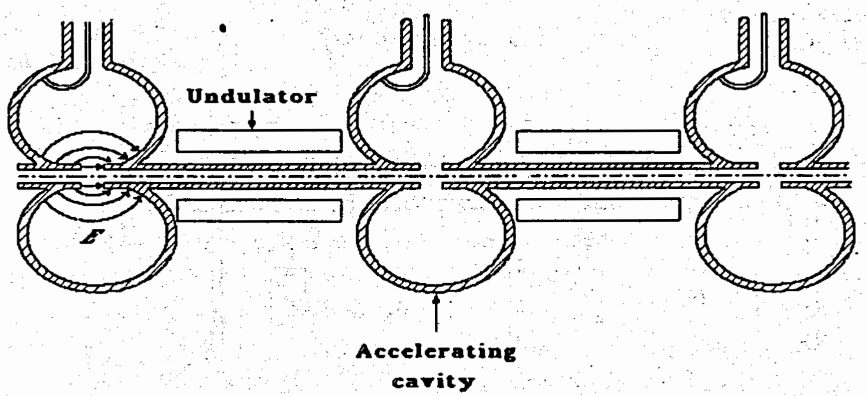

Figure 2: Scheme B: Sectional main undulator with separated accelerating cavities

In section 4 we proceed the consideration with scheme B. Peculiar feature of this scheme is that the main undulator is divided into pieces and short RF cavities with time-dependent RF fields are placed between them (see Fig.2). In this scheme the electron acceleration is performed discretely and processes of electron acceleration by the RF field and deceleration by the optical field are separated in space. This results in some decrease of the final efficiency with respect to the scheme A, nevertheless, as we will show below with numerical example, a high efficiency may be achieved, too. Moreover, this scheme is more preferable from technical point of view. There are no limitations on the undulator gap value and RF cavities may operate at the frequency of the driving accelerator (as a rule, at L- or S-band frequency) providing a high acceleration rate of the order of several tens MV/m.

The above mentioned schemes A and B need RF supplies for their operation. In section 5 we propose quite a novel scheme C which operates without a RF power supply. The main undulator of this scheme is fabricated with deep tapering (for instance, with decreasing magnetic field at fixed period, or with decreasing period at fixed undulator parameter). A tunable decelerating RF structure is installed inside the main undulator gap (see Fig.3). Initially it is tuned in such a way that the RF field, induced inside it by the electron beam, decelerates the electron beam keeping the resonance of electrons with the small optical field in the resonator along the undulator length. As a result, the optical field in the resonator begins to grow. To keep the resonance condition at higher values

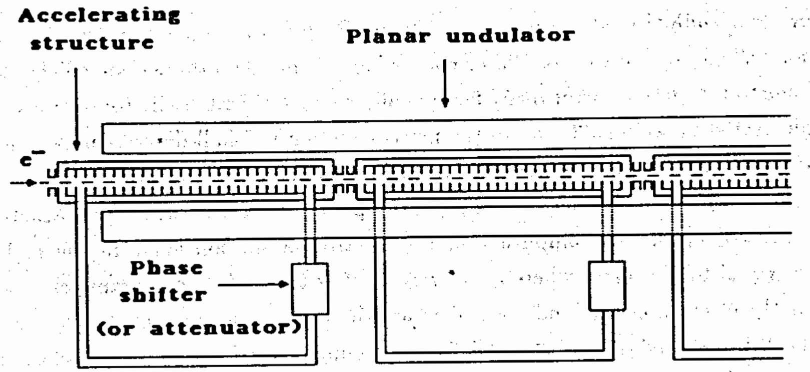

Figure 3: Scheme C: Tapered undulator with tunable decelerating RF structure

of the optical field, the decelerating RF structure is tuned in time in such a way that the induced RF fields are decreasing while the optical field in the resonator is increasing. Finally, the stationary mode of operation with high efficiency is settled when the induced RF field is small and deceleration of electrons is performed mainly by the optical field. Here we should note that the chosen value of the undulator tapering depth should provide the resonance condition of electrons with the optical field corresponding to this stationary mode of operation.

To realize the proposed scheme C, one should provide a change of resonance properties of the decelerating RF structure within a macropulse of the driving accelerator. One possible way of the technical realization, based on the travelling wave resonator technique, is considered in section 5. Here we should note only that this scheme seems to be extremely attractive, so as it does not require a RF power supply for its operation. RF structures operating at a shorter wavelength band, such as K_u–, K– or K_α-band may be used giving a possibility to decrease the undulator gap. As a result, the FEL scheme with the tunable decelerating RF structure reveals a possibility to construct high efficiency FEL oscillators of visible range.

2 Qualitative consideration

Basic assumptions. The present treatment is based on a one-dimensional FEL oscillator model. We assume an electron current pulse duration to be long and do not take into account longitudinal modes competition effects. Despite its simplicity such a model reveals main features of the FEL oscillator concerning the problem to increase efficiency. It enables one to take into account many factors influencing the FEL oscillator operation, which is illustrated in sections 3 – 5. In the present section we shall describe only basic features of the considered method and shall simplify a situation significantly.

An electron beam moves along the z axis of the planar undulator with the magnetic field $\vec{B} = \vec{e}_x B \cos(\kappa_w z)$. The amplitude of the electron oscillation angle in the main undulator is equal to $\theta = Q/\gamma$, where $Q = eB/\kappa_w mc^2$ is the undulator parameter, $\gamma = \mathcal{E}/mc^2$, $\mathcal{E}$ is the electron energy and $-e$ and m are the charge and mass of the electron, respectively. It is assumed that $\theta^2 \ll 1$ and the longitudinal electron velocity v_z is close to the velocity of light c. The amplitude of the electric field of the optical wave synchronous with the electron beam is of the form:

$$\vec{E} = \vec{e}_y \tilde{E} \exp[i\omega(z/c - t)] + C.C.,$$

where the lasing frequency ω is defined by the condition of maximum gain in the small-signal mode of operation. The particle motion is described by "energy-phase" variables with energy $\mathcal{E}$ as canonical momentum and phase $\psi = \kappa_w z + \omega(z/c - t)$ as canonically conjugated coordinate. In this representation the longitudinal coordinate z is an independent variable (see, e.g., refs. [17, 18]). To study the nonlinear mode of FEL oscillator operation we use the macroparticle method. We choose M macroparticles over a modulation density period, i.e. in phase interval from 0 to 2π. The equations of motion (averaged over the undulator period) may be written in the following reduced form [18] ($k = 1, \ldots, M$):

$$d\hat{P}_{(k)}/d\hat{z} = \hat{\varphi}\cos(\psi_{(k)} + \psi_s) + \hat{\varphi}_z, \quad (1a)$$

$$d\psi_{(k)}/d\hat{z} = \hat{P}_{(k)} + \hat{C}, \quad (1b)$$

where $\hat{z} = z/l_w$, l_w is the length of the main undulator, $\hat{P} = P/g\mathcal{E}_o$, $P = (\mathcal{E} - \mathcal{E}_o)$ is the energy deviation from the nominal value $\mathcal{E}_o$, $g = \gamma_{z0}^2 c/\omega l_w \simeq (4\pi N_w)^{-1}$, N_w is the number of the main undulator periods, $\hat{\varphi} = [JJ]_0 l_w \varphi/2g\mathcal{E}_o$ is the reduced amplitude of the effective potential of the electron interaction with the optical field, $\varphi \exp(i\psi_s) = -e\theta_o \tilde{E}$, $\theta_o = Q_o/\gamma_o$ is the electron oscillation angle, $Q_o = eB_o/\kappa_w mc^2$ is the undulator parameter at $z = 0$, $\gamma_{z0}^{-2} = \gamma_o^{-2} + \theta_o^2/2$, $[JJ]_o = J_0(\nu_o) - J_1(\nu_o)$ and $\nu_o = Q_o^2/4(1 + Q_o^2/2)$. The term $\hat{\varphi}_z = -eE_z l_w/g\mathcal{E}_o$ in the right-hand side of equation (1a) takes into account the action of the slowly changing amplitude of the external longitudinal RF field $E_z = E_z(z,t)$ which is introduced into the interaction region ($E_z < 0$). The term $\hat{C} = \hat{C}_o = [\kappa_w - \omega(1 + Q_o^2/2)/2c\gamma_o^2]l_w$ in the right-hand side of equation (1b) is the detuning parameter of particle with the nominal energy $\mathcal{E}_o$ from resonance at $z = 0$. When undulator tapering is performed by decreasing the magnetic field with $[B_o - B(z)]/B_o = \xi z$, then the detuning

parameter $\hat{C}$ depends on z as $\hat{C} = [\kappa_w - \omega(1 + Q^2(z)/2)/2c\gamma_o^2]l_w = \hat{C}_o + \hat{\xi}\hat{z}$, where $\hat{\xi} = \xi l_w Q_o^2/2g(1 + Q_o^2/2)$ and $\hat{C}_o$ is defined by the condition of maximum gain in the small-signal mode of operation. In this section we consider the simplified situation when the efficiency is increased significantly with respect to the conventional FEL oscillator scheme, but still remains much less than unity. It follows from this assumption that we can neglect the quadratic terms in the expression for the detuning parameter and the dependence on energy of Q and γ in amplitude factors.

From Maxwell's wave equation we get the reduced equations for the amplitude $\hat{\varphi}$ and the phase ψ_s of the effective potential of interaction:

$$d\hat{\varphi}/d\hat{z} = -2\beta M^{-1} \sum_{k=1}^{M} \cos(\psi_{(k)} + \psi_s), \quad (2a)$$

$$d\psi_s/d\hat{z} = -2\beta M^{-1} \hat{\varphi}^{-1} \sum_{k=1}^{M} \sin(\psi_{(k)} + \psi_s), \quad (2b)$$

where

$$\beta = \pi\theta_o^2 j\omega l_w^3 [JJ]_o^2 / 2c\gamma_{z0}^2 \gamma_o I_A$$

is the gain parameter, j is the beam current density and $I_A = mc^3/e \simeq 17$ kA. When calculating the beam current density j, entering into the expression for the gain parameter β, we assume that transverse dimensions of the electron beam are much less than the gaussian beam waist size w_o. As a result, in one-dimensional equations we substitute the beam current density by the effective value $j = 2\pi^{-1} w_o^{-2} I$, where I is the beam current. Here we do not take into account variation of the amplitude and the phase of the gaussian optical mode along the undulator axis.

The prebuncher is a short plane undulator with a number of periods N_p and is placed in front of the main undulator. As a rule, the magnetic field of the prebuncher undulator should be less than that of the main undulator. When choosing the prebuncher undulator parameters, the following condition should be fulfilled:

$$\lambda_p(1 + Q_p^2/2) \simeq \lambda_w(1 + Q_o^2/2),$$

where $\lambda_w = 2\pi/\kappa_w$ is the period of the main undulator, $\lambda_p = 2\pi/\kappa_p$ is the period of the prebuncher undulator, $Q_p = eB_p/\kappa_p mc^2$ and B_p is the prebuncher magnetic field. When writing down the equations for the prebuncher, it is convenient to perform their normalization to the parameters of the main undulator (the prebuncher reduced length is equal to $\hat{l} = l_p/l_w$):

$$d\hat{P}_{(k)}/d\hat{z} = b_1 \hat{\varphi}\cos(\psi_{(k)} + \psi_s), \quad (3a)$$

$$d\psi_{(k)}/d\hat{z} = b_2(\hat{P}_{(k)} + \hat{C}), \quad (3b)$$

$$d\hat{\varphi}/d\hat{z} = -2\beta M^{-1} b_1 \sum_{k=1}^{M} \cos(\psi_{(k)} + \psi_s), \tag{4a}$$

$$d\psi_s/d\hat{z} = -2\beta M^{-1} \hat{\varphi}^{-1} b_1 \sum_{k=1}^{M} \sin(\psi_{(k)} + \psi_s), \tag{4b}$$

where

$$b_1 = Q_p[JJ]_p/Q_o[JJ]_o, \qquad b_2 = (1 + Q_p^2/2)/(1 + Q_o^2/2),$$

$$[JJ]_p = J_0(\nu_p) - J_1(\nu_p), \qquad \nu_p = Q_p^2/4(1 + Q_p^2/2).$$

The prebuncher and the main undulator are separated with the drift space (or dispersion section). The change of the electron phase in the drift space is given with the following expression:

$$\Delta\psi_{(k)} = (\hat{C}_o + \hat{P}_{(k)})\hat{D} + \delta\psi, \tag{5}$$

where $\hat{D} = D/(1+Q_o^2/2)l_w$, D is the length of the drift section. The term $\delta\psi = -2\pi N_w \hat{D}$ takes into account the fact that the electron beam slippage length is not multiple to the radiation wavelength.

So, equations (1) – (5) enable one to calculate the field amplification $G = \Delta\hat{\varphi}/\hat{\varphi}$ per one pass of the undulator (in this section we assume $G \ll 1$). To take into account the resonator losses we use a phenomenological approach introducing the field damping factor K per one resonator round-trip (K is approximately equal to one half of the resonator power losses). The lasing takes place when the amplification in the small-signal mode of operation is greater than the dumping factor, $G_s > K$, and saturation takes place when G becomes equal to K.

If there is no external accelerating (or decelerating) RF field in the interaction region, the FEL efficiency is given with the expression $\eta = ec \mid \tilde{E}\Delta\tilde{E} \mid /\pi j \mathcal{E}_o$. It is convenient for the further representation to introduce the reduced efficiency $\hat{\eta} = \eta/g = \hat{G}\hat{\varphi}^2/2$, where $\hat{G} = G/\beta$. One can easily show that the conservation energy law takes place and the reduced FEL efficiency is equal to the averaged value of the reduced electron energy losses: $\hat{\eta} = -<\hat{P}>$. At the saturation we obtain:

$$\hat{\eta} = \hat{K}\hat{\varphi}^2/2,$$

where $\hat{K} = K/\beta$. It is useful to note that for a conventional scheme of the FEL oscillator with the homogeneous undulator, the maximal reduced FEL $\hat{\eta}_{(h)}$ is achieved at the optimal value of the reduced resonator losses $\hat{K} = \hat{K}_{opt} = 0.028$ [7, 8]:

$$\hat{\eta}_{(h)} = 3.62, \qquad \hat{K}_{opt} = 0.028. \tag{6}$$

In the presence of external RF field in the interaction region, the above definition of the efficiency becomes nonstrict (in fact, it may exceed the value of 100%). But such

a definition with normalization to the initial energy of electron is somewhat convenient when comparing the efficiency increase due to the introducing of the RF field with that of conventional FEL configuration. Thus, below we shall use this definition for the efficiency denoting it as $\eta_{(ie)}$ (initial energy) and remembering that the strict definition of the efficiency is given by the expression $\eta_{(f)} = ce \mid \tilde{E}\Delta\tilde{E} \mid /\pi j(\mathcal{E}_o + \Delta\mathcal{E})$, where $\Delta\mathcal{E}$ is the electron energy increase due to the interaction with the external RF field. At a constant gradient of the accelerating RF field, the reduced values corresponding to these two definitions of the efficiency are connected with the simple relation:

$$\hat{\eta}_{(f)} = \hat{\eta}_{(ie)}/(1 + g\hat{\varphi}_z).$$

Now, using the above mentioned assumptions, let us perform a brief qualitative study of the proposed FEL schemes A, B and C.

Scheme A: Accelerating structure combined with the main undulator. Let us consider a model situation when the electron beam density after the prebuncher can be approximated by a sequence of the δ - functions with the period $\lambda = 2\pi c/\omega$. The bunches are fed into the main undulator in an optimal decelerating phase of the effective potential (i.e. in equations (1) and (2) we let $\psi_{(1)} \simeq \pi$, $\psi_s \simeq 0$ and $M = 1$). The main undulator is untapered one ($\hat{\xi} = 0$) and the detuning parameter $\hat{C}_o$ is set equal to zero. It follows from equations (1) that the external RF field should be changed proportionally to the optical field value, $\hat{\varphi}_z(t) = S\hat{\varphi}(t)$, where $S \simeq 1$, to keep the resonance condition. In this case there is no phase motion of the bunches and we find from equation (2a) that the optical field increment per one undulator pass is equal to $\Delta\hat{\varphi} \simeq 2\beta$ which corresponds to the field amplification coefficient $G = \Delta\hat{\varphi}/\hat{\varphi} \simeq 2\beta/\hat{\varphi}$. The growth of the optical field is ceased at the stationary regime when the field amplification coefficient becomes equal to the field damping factor K. In the stationary regime, the optical field amplitude is equal to $\hat{\varphi} \simeq 2\beta/K = 2/\hat{K}$, the RF field amplitude is equal to $\hat{\varphi}_z \simeq 2/\hat{K}$ and the expressions for the FEL reduced efficiency are given by:

$$\hat{\eta}_{(ie)} \simeq 2\hat{K}^{-1}, \qquad \hat{\eta}_{(f)} \simeq 2(\hat{K} + 2g)^{-1}, \tag{7}$$

and the expressions for physical efficiency by:

$$\eta_{(ie)} \simeq (2\pi N_w \hat{K})^{-1}, \qquad \eta_{(f)} \simeq (2\pi N_w \hat{K} + 1)^{-1}.$$

Remembering that usually damping factor $\hat{K}$ is much less than unity, and that the reduced efficiency of the conventional FEL oscillator scheme is equal to $\hat{\eta}_{(h)} = 3.62$ (see expression (6)), we conclude that there may be a significant increase in the FEL efficiency when using the proposed FEL scheme.

To verify this qualitative consideration, we have performed a set of numerical simulations with a large number of macroparticles ($M = 100$) using equations (1) - (5). The optimization of the overall parameters has been performed to maximize the value of $\hat{\eta}_{(ie)}$. These experiments have confirmed the validity of the parametric dependence $\hat{\eta}_{(ie)} \propto \hat{K}^{-1}$ but have resulted in a smaller proportionality factor:

$$\hat{\eta}_{(ie)} \simeq 0.8\hat{K}^{-1}, \qquad \hat{\eta}_{(f)} \simeq 0.8(\hat{K}+g)^{-1}, \tag{8}$$

and for physical values:

$$\eta_{(ie)} \simeq (5\pi N_w \hat{K})^{-1}, \qquad \eta_{(f)} \simeq 0.8(4\pi N_w \hat{K}+1)^{-1}.$$

The simulations have shown that in the real situation the electron bunches have finite phase extent, their optimal phase at the entrance into the main undulator is less than π and coefficient S is less than unity.

Scheme B: Sectional main undulator with separated acclerating cavities. In this scheme the main undulator is divided into some number of pieces and short RF cavities are installed between them. Due to a variety of possible configurations, it is extremely difficult to obtain universal qualitative formulae for the efficiency calculation. Nevertheless, expressions (8) may be considered as an upper limit for the maximal attainable efficiency.

Scheme C: Tapered main undulator with tunable decelerating RF structure. This scheme uses the main undulator with the tapered parameters. For simlicity, let us consider the case of the linear undulator tapering when the detuning parameter is changed according to the law: $\hat{C} = \hat{C}_o + \hat{\xi}\hat{z}$. The parameters of the RF structure are chosen in such a way that at the initial moment of time the decelerating RF field induced by the electron beam results in $\hat{\varphi}_{zo} \simeq -\hat{\xi}$. In this case the phase motion of electrons is small and resonance of electrons with the optical fields takes place along the main undulator length. In the same way as has been mentioned above, we consider a model situation with the ideally bunched electron beam at the main undulator entrance. But contrary to the scheme A, we should decrease the value of the decelerating RF field during the process of the optical field growth:

$$\hat{\varphi}_z(t) \simeq -\hat{\xi} + S\hat{\varphi}(t),$$

where $S \simeq 1$. It is seen from equations (1) that the resonance of electrons with the optical field will be maintained during the process of the optical field growth up to the value $\hat{\varphi} \simeq \hat{\xi}$ when the RF field becomes equal to zero. When all the parameters are chosen to be optimal, i.e. at $\hat{\xi} \simeq 2\hat{K}^{-1}$, all the considerations performed for the scheme A are valid here, too. The only difference is that in the case under study the values $\hat{\eta}_{(ie)}$ and $\hat{\eta}_{(f)}$ are equal: $\hat{\eta}_{(ie)} = \hat{\eta}_{(f)} \simeq 2\hat{K}^{-1}$, because the induced RF field vanishes in the stationary mode

of operation. More precise relations given by the numerical simulation are still valid, too: $\hat{\eta}_{(ie)} = \hat{\eta}_{(f)} \simeq 0.8\hat{K}^{-1}$.

In conclusion of this section we would like to emphasize that all the proposed schemes use the prebuncher with fixed parameters. Simulations have shown that though the electron bunching in the prebuncher and the drift space depends on the amplitude of the radiation field stored in the resonator, the parameters of the prebuncher and the drift space may be chosen to be fixed to provide optimal bunching in the strong optical field corresponding to the stationary regime. Of course, at a small field amplitude in the resonator such a choice leads to nonoptimal bunching but this does not stop the optical field growth.

Simulations also have shown that the proposed FEL schemes provide a reliable operation in the presence of the finite initial energy spread of electrons in the beam. It takes place when, operating in the stationary regime, the prebuncher provides such a value of the energy modulation in the beam which is much larger than the initial energy spread, and is less than the trap depth of the ponderomotive well in the main undulator. The results of numerical simulations have shown that in real situations, when the energy spread is about some fraction of percent and the damping factor $\hat{K}$ is rather small, the efficiency does not decrease significantly with respect to the case of the "cold" electron beam. The influence of the initial energy spread and other factors decreasing the efficiency with respect to the values given by relation (8), are taken into account in the next sections where realistic numerical examples are presented.

3 Scheme A: Accelerating structure combined with the main undulator

This scheme is similar to that proposed in refs. [13, 14]. The only difference is that we propose a more realistic way to realize this scheme which is totally based on standard undulator and RF structure technology. We propose to use a standard undulator (for instance, a permanent magnet or hybrid one) with a conventional iris-loaded waveguide installed in its gap (see Fig.1). This accelerating structure is fed by the RF power source operating at a harmonic frequency of the driving accelerator and is synchronized with the RF power system of the latter. Successful operation of this scheme takes place when the accelerating rate in the accelerating structure is proportional to the optical field amplitude in the resonator. It may be achieved, for instance, by introducing of the feedback from the optical field detector to the RF power supply.

Another important problem is that of the choice of optimal RF band. First, to minimize the size of the undulator gap, one should minimize the transverse dimensions of

Table 1. Scheme A: Accelerating structure combined with the main undulator

Electron beam	
Energy, $\mathcal{E}_o$	50 MeV
Peak current, I	110 A
Average macropulse current, I_a	20 mA
Micropulse duration	5 ps
Energy spread, $\sigma/\mathcal{E}_o$	0.5 %
Magnetic system	
Prebuncher	
Period, λ_p	9 cm
Magnetic field, B_p	0.49 kG
Number of periods, N_p	3
Length of drift space, D	39 cm
Main undulator	
Period, λ_w	6 cm
Magnetic field, B_w	2 kG
Number of periods, N_w	30
Optical resonator	
Wavelength, λ	5 μm
Rayleigh length, z_R	90 cm
Total power losses	2 %
Reaccelerating system	
RF frequency	8 GHz
Number of sections	4
Section length, l_s	40 cm
Structure type	$\pi/2$
Iris aperture radius, a	4 mm
Cell radius, b	13.3 mm
Reduced shunt impedance, R_s	94 MΩ/m
Attenuation constant, α	0.74 m^{-1}
Group velocity, v_g/c	0.021
RF power per section	1 MW
Maximal accelerating gradient, $\mid E_{z0} \mid$	11.8 MV/m

the waveguide by choosing as short RF wavelength as possible. On the other hand, there should exist high peak power RF amplifiers (with output power $W_{peak} \geq 1$ MW) with a sufficiently long pulse duration (several microseconds or more) corresponding to that of the driving accelerator. Analysis of the present-day situation with RF sources shows that the most appropriate band for this purpose is the X-band. For instance, the Varian X3030 klystron operates in a CW mode at 8 GHz frequency with an output power ~ 1 MW. Below, when considering a numerical example, we will use the parameters of this klystron.

During the last years there are significant achievements in the development of the X-band accelerating structure technology. This branch of accelerating technique R&D has been developed intensively due to the needs of future generation linear colliders and now there is no problems to fabricate travelling wave X-band structure with transverse dimensions of about 3 cm. Though these dimensions are rather large, resulting in a choice of a large undulator period (and in a larger radiation wavelength at a fixed electron beam energy), the scheme proposed seems to be extremely attractive providing the high FEL efficiency.

Let us now proceed with numerical example (see Table 1). The RF structure is a conventional iris-loaded waveguide of outer diameter $2b \simeq 2.7$ cm. To provide its cooling, the size of the undulator gap is chosen to be 3.5 cm. The chosen value of the peak magnetic field is slightly less than that given by the Halbach formula for hybrid SmCo magnets [19]. Each of the four accelerating sections is fed by the Varian X3030 klystron.

When considering this scheme one should take into account possible diffraction losses due to the small size of the waveguide iris aperture. In the example considered the Fresnel number is equal to $N_F = a^2/\lambda l_w = 1.8$ and diffraction losses may be neglected. Second, electron bunch slippage with respect to the optical bunch $N_w\lambda = 0.15$ mm is much less than the electron bunch length, so this effects is negligible, too. Another harmful effect may be connected with the finite phase extent of the electron bunch with respect to the RF wavelength used in the reaccelerating RF structure. In the example considered the energy deviation due to this effect is much less than the initial energy spread of electrons in the beam.

To be more strict, here we perform a more detailed analysis than that presented in section 2 taking into account the axial variation of the amplitude and phase of the gaussian TEM_{00} of the optical resonator, axial inhomogeneity of the RF accelerating field, etc. So, equations (3) and (4) describing the particle motion and field amplification in the prebuncher are written in the following form:

$$d\hat{P}_{(k)}/d\hat{z} = f_A b_1 \hat{\varphi} \cos(\psi_{(k)} + \psi_s - f_\psi), \qquad (9a)$$

$$d\psi_{(k)}/d\hat{z} = b_2(\hat{P}_{(k)} + \hat{C}_o), \qquad (9b)$$

$$d\hat{\varphi}/d\hat{z} = -2\beta M^{-1} f_A b_1 \sum_{k=1}^{M} \cos(\psi_{(k)} + \psi_s - f_\psi), \qquad (10a)$$

$$d\psi_s/d\hat{z} = -2\beta M^{-1} \hat{\varphi}^{-1} f_A b_1 \sum_{k=1}^{M} \sin(\psi_{(k)} + \psi_s - f_\psi), \qquad (10b)$$

where functions $f_A(\hat{z})$ and $f_\psi(\hat{z})$ reflect the change of the amplitude and the phase of the gaussian TEM_{00} of the optical resonator and the other notations are similar to those introduced in section 2.

The change of the electron phase in the drift space, i.e. at $\hat{z} = \hat{l}_p$, is given with expression (5).

Equations (1) and (2) describing the particle motion and field amplification in the main undulator are written in the following form :

$$d\hat{P}_{(k)}/d\hat{z} = (1 + g\hat{P}_{(k)})^{-1} f_A \hat{\varphi} \cos(\psi_{(k)} + \psi_s - f_\psi) + \hat{\varphi}_z, \qquad (11a)$$

$$d\psi_{(k)}/d\hat{z} = \hat{C}_o + (1 + g\hat{P}_{(k)})^{-2} \hat{P}_{(k)} (1 + 0.5 g\hat{P}_{(k)}), \qquad (11b)$$

$$d\hat{\varphi}/d\hat{z} = -2\beta M^{-1} f_A \sum_{k=1}^{M} (1 + g\hat{P}_{(k)})^{-1} \cos(\psi_{(k)} + \psi_s - f_\psi), \qquad (12a)$$

$$d\psi_s/d\hat{z} = -2\beta M^{-1} \hat{\varphi}^{-1} f_A \sum_{k=1}^{M} (1 + g\hat{P}_{(k)})^{-1} \sin(\psi_{(k)} + \psi_s - f_\psi). \qquad (12b)$$

In the accepted notations $\hat{z}_i = \hat{l}_p$ and $\hat{z}_f = (\hat{l}_p + 1)$ are the coordinates of the main undulator entrance and exit, respectively. Factor $(1 + g\hat{P}_{(k)}) = \mathcal{E}/\mathcal{E}_o$ reflects the dependence of the electron oscillation angle θ on energy (see, e.g., ref. [18]). The gaussian beam waist is assumed to be placed in the middle of the main undulator at $\hat{l}_p + 0.5$ and the Rayleigh length is assumed to be equal to the main undulator half-length $\hat{z}_R = 0.5$. So, the amplitude and phase functions of the gaussian optical mode $f_A(\hat{z})$ and $f_\psi(\hat{z})$, entering into equations (9) - (12) are given with the expressions:

$$f_A = [1 + (\Delta\hat{z}/\hat{z}_R)^2]^{-1/2}, \qquad f_\psi = \text{arctg}(\Delta\hat{z}/\hat{z}_R),$$

where $\Delta\hat{z} = -(\hat{l}_p + 0.5 - \hat{z})$ for the main undulator and $\Delta\hat{z} = -[\hat{l}_p + 0.5 - \hat{z} + \hat{D}(1 + Q_o^2/2)]$ for the prebuncher.

When performing simulations, we have taken into account that there should be technical clearance between the sections equal to $\Delta z = 6.6$ cm (or in normalized notations $\Delta\hat{z} = 0.03$). In addition, the algorithm used takes into account the dependence on the axial coordinate of the RF accelerating field due to the waveguide losses and electron beam load:

$$E_z(z,t) = E_{z0}(t)\exp[-\alpha(z - z_j)] + I_a R_s\{1 - \exp[-\alpha(z - z_j)]\},$$

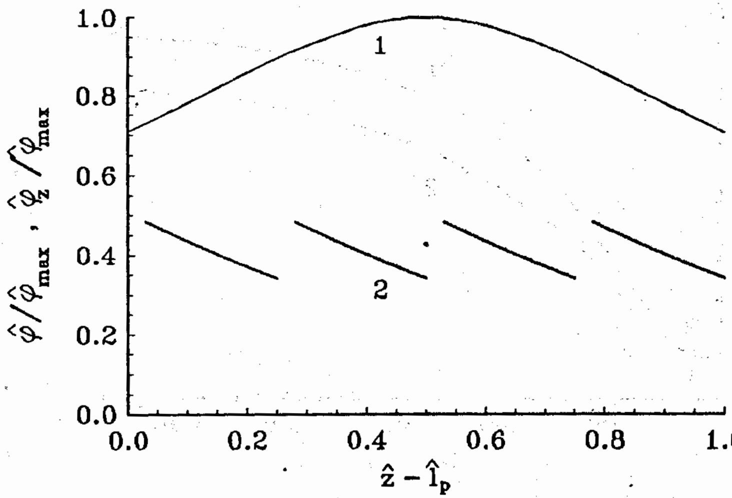

Figure 4: Stationary mode of operation (scheme A): (1) – relative distributions of optical field and (2) – accelerating RF field along the main undulator axis

where z_j is the coordinate of the j-th section ($E_{z0} < 0$ and $I_a > 0$). As a result, the expression for the normalized value of the RF field in the j-th accelerating section takes the form ($\hat{z}_j \leq \hat{z} \leq \hat{z}_j + 0.22$):

$$\hat{\varphi}_z = \hat{\varphi}_{z0}(t)\exp[-\hat{\alpha}(\hat{z} - \hat{z}_j)] + \hat{\varphi}_i\{1 - \exp[-\hat{\alpha}(\hat{z} - \hat{z}_j)]\}, \qquad (13)$$

where

$$\hat{\varphi}_{z0} = -4\pi N_w e E_{z0} l_w/\mathcal{E}_o, \qquad \hat{\varphi}_i = -4\pi N_w e I_a R_s/\mathcal{E}_o,$$

$\hat{\varphi}_{zo} > 0$, $\hat{\varphi}_i < 0$, $\hat{\alpha} = \alpha l_w$ and the coordinates of the RF sections $\hat{z}_j$ take the following values:

$$\hat{z}_1 = \hat{l}_p + 0.03, \qquad \hat{z}_2 = \hat{l}_p + 0.28, \qquad \hat{z}_3 = \hat{l}_p + 0.53, \qquad \hat{z}_4 = \hat{l}_p + 0.78.$$

In the process of simulations the following relation has been maintained: $\hat{\varphi}_{z0}(t) = S\hat{\varphi}(t)$. Fig.4 shows relative axial distributions of the RF and optical fields along the main undulator axis.

The energy spread at the prebuncher entrance is assumed to be a Gaussian with the distribution function

$$F(P) = (2\pi\sigma^2)^{-1/2}\exp(-P^2/2\sigma^2)$$

which corresponds to the distribution function over reduced energy deviation

$$\hat{F}(\hat{P}) = (2\pi\hat{\Lambda}_T^2)^{-1/2}\exp(-\hat{P}^2/2\hat{\Lambda}_T^2),$$

where $\hat{\Lambda}_T = 4\pi N_w \sigma/\mathcal{E}_o$ is the energy spread parameter.

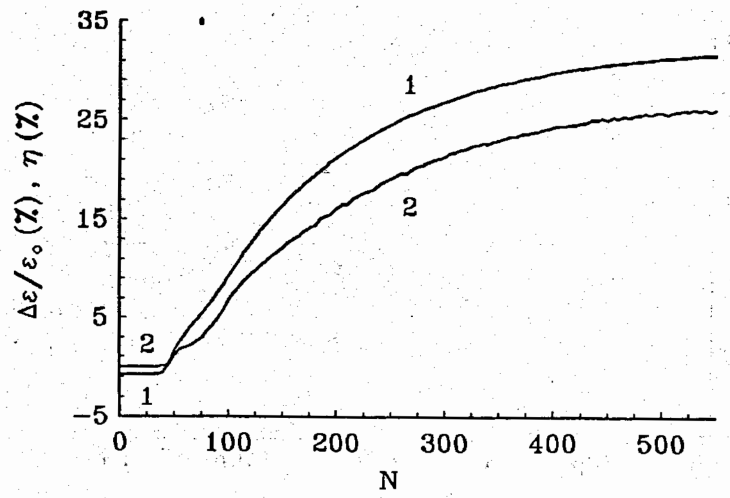

Figure 5: Scheme A: (1) – electron energy increment $\Delta\mathcal{E}/\mathcal{E}_o$ due to the action of RF field and (2) – the FEL efficiency $\eta_{(ie)}$ versus the number of resonator round-trips

Using the above mentioned notations and physical parameters from Table 1, we find that the corresponding reduced parameters are as follows: $\beta = 5.8$, $g = 2.65 \times 10^{-3}$, $\hat{K} = 1.7 \times 10^{-3}$, $\hat{\Lambda}_T^2 = 3.55$, $\hat{l}_p = 0.15$, $b_1 = 0.4$, $b_2 = 0.67$, $\hat{D} = 0.13$, $\delta\psi = -0.2$, $\hat{C}_o = 5.9$, $S = 0.485$, $\hat{\varphi}_i = -25.4$. The initial detuning $\hat{C}_o$ is defined by the condition of maximal small-signal gain when there is no external RF field.

The presented FEL oscillator scheme operates as follows. At the initial moment of time $t = 0$ the RF power supply is turned off and the optical field is growing in time as it occurs in the conventional FEL oscillator configuration. Then, as far as optical field is growing, the amplitude of the RF accelerating field is increasing proportionally to the optical one. When the optical field amplification becomes equal to resonator losses, the stationary regime of operation with high efficiency is settled.

In the numerical example considered all the paprameters are chosen in such a way that the final value of the accelerating RF field is achieved at maximal level of the klystron output power. Fig.5 presents the dependencies on the number of resonator round-trips of electron energy increment $\Delta\mathcal{E}/\mathcal{E}_o$ due to the action of the RF field and of the FEL efficiency $\eta_{(ie)}$. In the stationary regime of operation we obtain $\eta_{(ie)} \simeq 26\%$ and $\eta_{(f)} \simeq 20\%$. One can find that these values for the FEL efficiency, obtained with taking into account many factors decreasing the efficiency, are visibly less than those given by qualitative estimations (8). Nevertheless, even in such a situation, a significant fraction of electrons is trapped in the regime of coherent deceleration resulting in a high efficiency.

In conclusion of this section we should note that a higher efficiency may be achieved using a more powerful klystron , a longer undulator and a greater number of accelerating sections. In the example considered we have chosen a relatively moderate value of the average beam current. Increasing of the value of the average beam current will lead to a significant increase of axial inhomogeneity of the RF field which will result in the efficiency decrease. To overcome this problem, standing wave accelerator sections may be used rather than travelling wave ones, or a greater number of shorter RF sections may be installed.

4 Scheme B: Sectional main undulator with separated accelerating cavities

It was shown in the previous section that the approach to increase the FEL oscillator efficiency by introducing accelerating RF fields into the interaction region, has limited possibilities due to severe technical limitations. The main problem is that of reducing the value of the undulator gap, so as peak field at the undulator axis depends exponentially on the gap value. As a result, it requires a necessity to develop novel types of undulator and RF structures [13, 14, 20], or to use accelerating RF structures operating at a small RF wavelength (see section 2).

In this section we consider another possibility to overcome this problem. We propose to use sectional main undulator and to install RF cavities between the undulator sections (see Fig.2). So as there is no limitation on transverse dimensions of the accelerating cavities, they may operate at the same frequency as the driving accelerator (*L*- or *S*-band) and provide a high accelerating gradient of about several tens MV/m. Of course, such a separation in space of the electron beam acceleration in the RF field and deceleration in the optical field possesses some disadvantages with respect to the scheme with combined functions. First, due to the finite energy spread of electrons in the beam, additional phase debunching takes place in the space between the undulator sections. Second, phase shift of electrons in the space between the undulator sections with respect to optical field phase, and phase motion of electrons trapped into the ponderomotive well are changed while the RF field amplitude is changed. These effects lead to detrapping of electrons and result in efficiency decrease. Nevertheless, the results of numerical simulations have shown that this scheme may provide the efficiency of about $10 \div 20\%$ which is much higher than that of the conventional FEL oscillator configuration. This scheme seems to be extremely attractive, so as it may be realized at the present level acceleration technique R&D.

Let us illustrate with a numerical example the possibilities of the proposed scheme

Table 2. Scheme B: Sectional main undulator with separated accelerating cavities

Electron beam	
Energy, $\mathcal{E}_o$	35 MeV
Peak current, I	35 A
Energy spread, $\sigma/\mathcal{E}_o$	0.2 %
Magnetic system	
Prebuncher	
Period, λ_p	9.2 cm
Magnetic field, B_p	0.44 kG
Number of periods, N_p	3
Length of drift space, D	36 cm
Main undulator	
Period, λ_w	5 cm
Magnetic field, B_w	3 kG
Number of sections	5
Spacing between sections	10 cm
Number of periods, N_w	50
Optical resonator	
Wavelength, λ	10 μm
Rayleigh length, z_R	145 cm
Total power losses	2 %
Reaccelerating system	
Number of cavities	4
maximal energy increment per cavity	1.9 MeV

(see Table 2). The chosen parameters of the RF cavities and RF power supply are in the limits of the present possibilities of acceleration technique and we will not discuss them here. We should note only that the chosen axial size of the RF cavity $l = 10$ cm provides the phase slippage $\simeq 2\pi$ of the optical wave with respect to the electron beam. When performing numerical simulations, we use equations (5) and (9) - (12) with the only exception that the term $\hat{\varphi}_z$ is excluded in the right-hand side of equation (11a). To describe particle motion in the cavities, we use the following equations:

$$\Delta\hat{P}_{(k)} = \hat{\varphi}_z\hat{d}, \tag{14a}$$

$$\Delta\psi_{(k)} = (\hat{C}_o + \hat{P}^{(in)}_{(k)})\hat{d} + \delta\psi + 0.5\hat{\varphi}_z\hat{d}^2, \tag{14b}$$

where $\Delta\hat{P}_{(k)} = \hat{P}^{(out)}_{(k)} - \hat{P}^{(in)}_{(k)}$, $\hat{P}^{(in)}_{(k)}$ and $\hat{P}^{(out)}_{(k)}$ are reduced energy deviations at the cavity entrance and exit, respectively, $\hat{d} = d/(1+Q_o^2/2)l_w$ is reduced cavity length, $\delta\psi = -2\pi N_w\hat{d}$, l_w is total undulator length (excluding spaces for cavities), $\hat{\varphi}_z(t) = -4\pi N_w e E_z(t) l_w(1+Q_o^2/2)/\mathcal{E}_o$, $\hat{\varphi}_z > 0$. The accelerating RF field in the cavities is assumed to be independent of axial coordinate and its amplitude grows in time proportionally to the optical field amplitude: $\hat{\varphi}_z(t) = S\hat{\varphi}(t)$. The amplitude and phase functions of the gaussian optical mode $f_A(\hat{z})$ and $f_\psi(\hat{z})$, entering equations (9) - (12) are calculated taking into account the finite length of accelerating cavities.

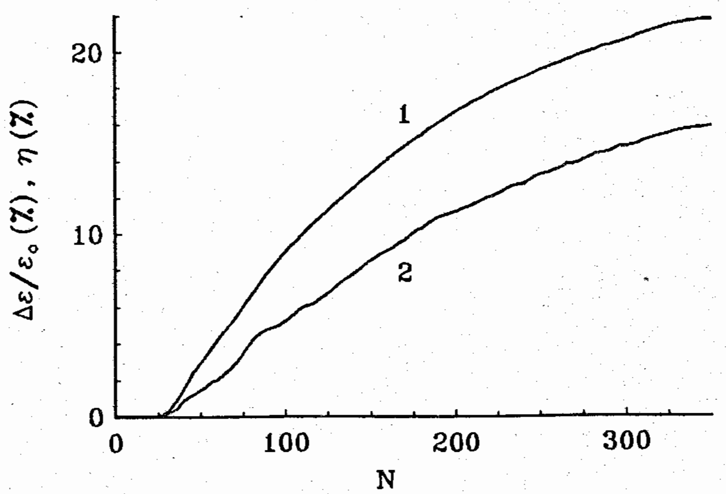

Figure 6: Scheme B: (1) – electron energy increment $\Delta\mathcal{E}/\mathcal{E}_o$ due to the action of RF field and (2) – the FEL efficiency $\eta_{(ie)}$ versus the number of resonator round-trips

The reduced parameters, corresponding to the physical parameters from Table 2, are as follows: $\beta = 7$, $g = 1.6 \times 10^{-3}$, $\hat{K} = 1.43 \times 10^{-3}$, $\hat{\Lambda}_T^2 = 1.58$, $\hat{l}_p = 0.11$, $b_1 = 0.31$,

$b_2 = 0.54$, $\hat{D} = 0.073$, $\delta\psi = 2.1$, $\hat{d} = 0.02$, $\hat{C}_o = 4$ and $S = 4.9$. Fig.6 presents the dependencies on the number of resonator round-trips of the electron energy increment $\Delta\mathcal{E}/\mathcal{E}_o$ due to the action of the RF field and of the FEL efficiency $\eta_{(ie)}$. In the stationary regime of operation we obtain $\eta_{(ie)} \simeq 16\%$ and $\eta_{(f)} \simeq 13\%$.

5 Scheme C: Tapered undulator with tunable decelerating RF structure

In this section we study a novel scheme to increase the FEL oscillator efficiency exploiting the time-dependent RF field technique. The proposed scheme consists of the prebuncher, the main undulator with tapered parameters and one or more tunable decelerating RF structures placed inside the gap of the main undulator (see Fig.3). A peculiar feature of the RF structure used is that it decelerates the electron beam by the self-induced RF field. Initially it is tuned in such a way to provide deceleration of electrons in accordance with the undulator tapering and exact resonance of electrons with the optical field takes place along the total undulator length. While the optical field is increasing, the RF structure is detuned to decrease the induced RF field and to sustain the resonance condition. Finally, when the optical field gain becomes equal to the resonator losses, the stationary regime with high efficiency is settled. The induced RF field is small in the stationary regime.

The advantage of the scheme with the tapered undulator and tunable decelerating RF structure is evident. It does not require RF power supply, so a shorter RF band may be chosen (K_u-, K- or K_α-band) giving a possibility to place the RF structure in a smaller undulator gap. As a result, a shorter undulator period may be used to generate the radiation with a shorter wavelength.

The key problem of the proposed scheme design is the problem of tuning the RF structure: its resonant properties should change significantly within the macropulse duration of the driving accelerator. There are several technical solutions and here we study in detail one of them, namely that using the travelling wave resonator technique (see, e.g., refs. [21, 22]). It is arranged as follows. The decelerating RF structure is a conventional iris-loaded waveguide. Its exit and entrance are connected with the homogeneous waveguide (transmitting waveguide). Thus, such a configuration forms a so called travelling wave resonant ring. When ohmic losses in the waveguides are small and phase shift of the RF wave per one round-trip is multiple to 2π, the energy losses of the electron beam in the iris-loaded waveguide may be increased significantly. The expression for decelerating RF field in the iris-loaded waveguide is of the form:

$$E_z = I_a R_s[[1 - \exp(-\alpha z)] + \delta\exp(-\alpha z)[1 - \exp(-\alpha l_s)]/[1 - \delta\exp(-\alpha l_s)]], \qquad (15)$$

where I_a is the average beam current, R_s is the shunt impedance, α is the attenuation constant and l_s is the length of the iris-loaded waveguide. Parameter δ is the transmission coefficient describing the feedback from the exit to the entrance of the iris-loaded waveguide and takes into account RF power losses, phase shift in the transmitting waveguide and steering elements. At exact resonance δ is a real number less than unity. When δ is a complex number, it means that frequency detuning takes place. Steering the amplitude and phase of the transmission coefficient δ, makes it possible to change the decelerating RF field in the iris-loaded waveguide.

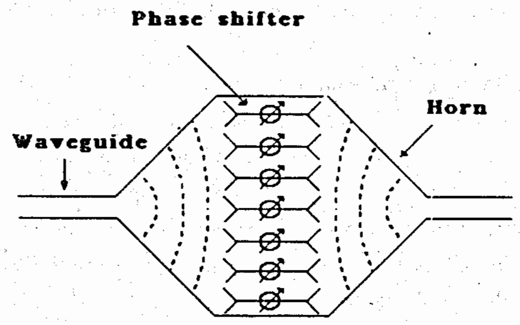

Figure 7: Scheme C: Phase shifter on the base of phased array antenna

There are several possibilities to provide such a steering. Here we consider one of them using technique of an array of fast phase shifters with reactive power divider of optical type. This technique is widely used to construct phased array antennas [23]. Usually $p-i-n$ diodes are used as phase shifters. In this scheme, the transmitting waveguide is divided into two parts and each half of the waveguide is matched with a horn (transmitting and receiving) to reduce the RF power flux (see Fig.7). At the exit of the transmitting horn, a feed-through array is installed which consists of receiving and transmitting radiating elements connected by phase shifters. Transverse dimensions of the phase shifters must be less than $\lambda_{rf}/2 \times \lambda_{rf}/2$ which enables one to place them inside each antenna element. The wave radiated by the phased array is received by the second horn which is placed next to the latter. The number of phase shifters in the phased array is defined by the maximal permissible value of the peak RF power for one diode and the total power circulating in the resonator. For instance, when these values are 100 W and 1 MW, respectively, 10^4 diodes should be installed in the phased array. As a result, at

$\lambda_{rf} \simeq 1$ cm transverse dimensions of the phased array will be about 50×50 cm and power losses due to the diode shifters will be about 0.3 dB per one resonator round-trip.

In this scheme the phased array performs two important functions. First, it steers the phase shift of the wave in the transmitting waveguide (and transmitting coefficient δ). Second, it matches the transmitting and receiving horns, thus eliminating RF power losses during the steering process.

Of course, there may exist other ways to steer the transmission coefficient δ. For instance, the amplitude of δ may be steered by the gas discharger [24], fast mechanical tuning may be used, etc. Here a peculiar feature of the travelling wave resonator may be used: when reflections in the resonator are greater than attenuation in the iris-loaded waveguide, the quality factor Q of the resonator depends significantly on the value of the reflections [22].

Let us now proceed with numerical example (see Table 3). One can easily obtain that all the requirements on the electron bunch length, waveguide iris aperture, etc., are in the limits of the model accepted (see section 3). RF deceleration system consists of 8 iris-loaded waveguides with parameters close to those accepted in the CLIC (CERN LInear Collider) project [25]. When using such a waveguide, the undulator gap may be chosen to be equal to 14 mm. The chosen value of the peak magnetic field is slightly less than that given by the Halbach formula for hybrid SmCo magnets [19] and the tapering of the main undulator is performed by decreasing the magnetic field at a fixed undulator period.

To describe the self-consistent process of amplification in the prebuncher and drift space, equations (9), (10) and (5) are used. Taking into account the undulator tapering, we rewrite the equations for the main undulator in the form [18]:

$$d\hat{P}_{(k)}/d\hat{z} = (1 + g\hat{P}_{(k)})^{-1}(1 - b_3 T) f_{JJ} f_A \hat{\varphi} \cos(\psi_{(k)} + \psi_s - f_\psi) + \hat{\varphi}_z,$$

$$d\psi_{(k)}/d\hat{z} = \hat{C}_o + (1 + g\hat{P}_{(k)})^{-2}[\hat{P}_{(k)}(1 + 0.5g\hat{P}_{(k)}) + T(1 - 0.5b_3 T)],$$

$$d\hat{\varphi}/d\hat{z} = -2\beta M^{-1}(1 - b_3 T) f_{JJ} f_A \sum_{k=1}^{M} (1 + g\hat{P}_{(k)})^{-1} \cos(\psi_{(k)} + \psi_s - f_\psi),$$

$$d\psi_s/d\hat{z} = -2\beta M^{-1}\hat{\varphi}^{-1}(1 - b_3 T) f_{JJ} f_A \sum_{k=1}^{M} (1 + g\hat{P}_{(k)})^{-1} \sin(\psi_{(k)} + \psi_s - f_\psi).$$

where $b_3 = 2g(1 + Q_o^2/2)/Q_o^2$, Q_o is the undulator parameter at the undulator entrance. All the notations are similar to those taken in section 3 with the following exceptions. The term $f_{JJ} = [JJ]/[JJ]_0$ takes into account the change of the factor $[JJ]$ due to the tapering. The term $T = T(\hat{z})$ describes the undulator tapering. We have chosen the parabolic law of tapering : $T(\hat{z}) = \hat{\xi}_1(\hat{z} - \hat{z}_o) + \hat{\xi}_2(\hat{z} - \hat{z}_o)^2$, where $\hat{z}_o = \hat{l}_p$ is the axial

Table 3. Scheme C: Tapered undulator with tunable decelerating RF structure

Electron beam	
Energy, $\mathcal{E}_o$	120 MeV
Peak current, I	55 A
Average macropulse current, I_a	200 mA
Micropulse duration	1 ps
Energy spread, $\sigma/\mathcal{E}_o$	0.2 %
Magnetic system	
Prebuncher	
Period, λ_p	6.3 cm
Magnetic field, B_p	0.94 kG
Number of periods, N_p	4
Length of drift space, D	70 cm
Main undulator	
Period, λ_w	3.5 cm
Magnetic field, B_w	4.5 kG
Number of periods, N_w	80
Tapering depth (parabolic), $\Delta B/B_o$	74 %
Optical resonator	
Wavelength, λ	0.65 μm
Rayleigh length, z_R	140 cm
Total power losses	2 %
Decelerating system	
RF frequency	30 GHz
Number of sections	8
Section length, l_s	25 cm
Structure type	$2\pi/3$
Iris aperture radius, a	2 mm
Cell radius, b	4.35 mm
Reduced shunt impedance, R_s	110 MΩ/m
Attenuation constant, α	1 m^{-1}
Group velocity, v_g/c	0.082

coordinate of the main undulator entrance and

$$\hat{\xi}_1 = \xi_1 l_w Q_o^2/2g(1+Q_o^2/2), \qquad \hat{\xi}_2 = \xi_2 l_w^2 Q_o^2/2g(1+Q_o^2/2).$$

The coefficients ξ_1 and ξ_2 are the linear and quadratic coefficients of the magnetic field tapering, respectively :

$$[B_o - B(z)]/B_o = \xi_1(z-z_o) + \xi_2(z-z_o)^2.$$

In the the example considered, these coefficients are chosen to be equal to $\xi_1 = 0.62$ and $\xi_1 = 0.12$, respectively. It should be noted that the parabolic law of the undulator tapering is more preferable with respect to the linear one.

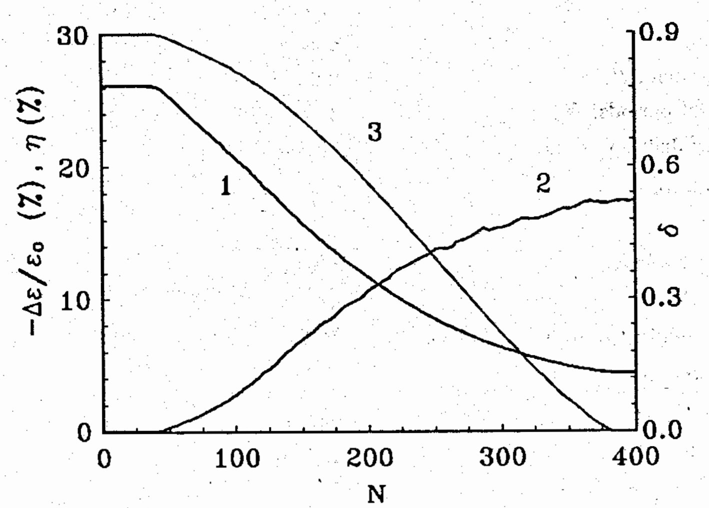

Figure 8: Scheme C: (1) – electron energy losses $\Delta\mathcal{E}/\mathcal{E}_o$ due to the action of induced RF field, (2) – the FEL efficiency η and (3) – transmission coefficient δ versus the number of resonator round-trips

When performing simulations, we have taken into account that there should be technical clearance between the RF sections equal to $\Delta z = 5.7$ cm (or in normalized notations $\Delta\hat{z} = 0.02$). In addition, the algorithm used takes into account the dependence on the axial coordinate of the RF decelerating field ($\hat{z}_j \le \hat{z} \le \hat{z}_j + 0.09, j = 1,\ldots,8$):

$$\hat{\varphi}_z = \hat{\varphi}_{z0}[1 - [1 - 0.22 \quad \delta/(1 \quad - \quad 0.78 \quad \delta)\}\exp[-2.8(\hat{z}-\hat{z}_j)]],$$

where $\hat{\varphi}_{z0} = -4\pi N_w e I_a R_s l_w/\mathcal{E}_o$. In the example considered $\hat{\varphi}_{z0} = -516$. The initial value of the transmission coefficient is equal $\delta = 0.9$ which corresponds to the maximal decelerating gradient 16 MV/m and electron energy losses 3.9 MeV per one section. During

simulations, the transmittion coefficient was changed to keep at the approximately constant level the total electron energy losses due to the action of the induced RF field and optical field:

$$\delta(t) = [0.9 - S\hat{\varphi}(t)][1 - 0.78S\hat{\varphi}(t)]^{-1}.$$

All the parameters are chosen in such a way that in the stationary regime with high efficiency the following relation takes place: $S\hat{\varphi} \simeq 0.9$. It means that in this case the transmission coefficient is close to zero and the induced decelerating RF field is small.

The reduced parameters, corresponding to the physical parameters from Table 3, are as follows: $\beta = 11$, $g = 10^{-3}$, $\hat{K} = 9.1 \times 10^{-4}$, $\hat{\Lambda}_T^2 = 4$, $\hat{l}_p = 0.09$, $b_1 = 0.42$, $b_2 = 0.56$, $b_3 = 1.94 \times 10^{-3}$, $\hat{D} = 0.12$, $\delta\psi = 1$, $\hat{C}_o = 0.6$, $\hat{\xi}_1 = 320$, $\hat{\xi}_2 = 60$, $S = 1.5 \times 10^{-3}$. Fig.8 presents the dependencies on the number of resonator round-trips of the electron energy losses $\Delta\mathcal{E}/\mathcal{E}_o$ due to the action of the induced RF field, of the FEL efficiency η and of the transmission coefficient δ. In the stationary regime of operation we obtain $\eta \simeq 17.5\%$.

6 Conclusion

In the present paper we have performed a detailed study of a possibility to use the time-dependent RF field to increase the FEL oscillator efficiency. The main emphasis was put on a problem to find such FEL schemes which may be realized at the present level of acceleration technique R&D. Three novel FEL oscillator schemes have been proposed wherein three different methods to introduce the time-dependent RF field into the interaction region are used. Another common feature of the schemes considered consists in the use of the prebuncher and drift space to increase the FEL oscillator efficiency.

Thorough study of the proposed schemes has been performed in the framework of one-dimensional FEL oscillator model and similarity laws describing the principles of operation of these FEL schemes were obtained.

It was shown that practical realization of the FEL oscillators with an efficiency of about 20% is quite feasible at the present level of acceleration technique R&D using standard undulator and RF structure technology.

Acknowledgments

We are extremely grateful to Prof. V.P. Sarantsev for support to our work. We also would like to thank Yu.N. Ulyanov for many useful discussions and recommendations.

References

[1] D.A.G. Deacon et al., Phys. Rev. Lett. **38**(1977)892

[2] P. Sprangle, C.M. Tang and W.M. Manheimer, Phys. Rev. Lett. **43**(1979)1932

[3] N.M. Kroll, P.L. Morton and M.N. Rosenbluth, IEEE J. Quantum. Electron. **QE-17**(1981)1436

[4] P. Sprangle, C.M. Tang and W.M. Manheimer, Phys.Rev. **A21**(1980)302

[5] D. Prosnitz, A. Szoke and V.K. Neil, Phys.Rev. **A21**(1981)1436

[6] T.J. Orzechowski et al., Phys. Rev. Lett. **57**(1986)2172

[7] B.W.J. McNeil, Nucl. Instrum. and Methods **A296**(1990)388

[8] E.L. Saldin, E.A. Schneidmiller and M.V. Yurkov, Optics Communications, **102**(1993)360

[9] D.W. Feldman et al., Nucl. Instrum. and Methods **A285**(1989)11

[10] E.L. Saldin, E.A. Schneidmiller and M.V. Yurkov, "The features of a FEL oscillator with a tapered undulator", Optics Communications, 1993

[11] E.M. McMillan, Phys. Rev. **68**(1945)143

[12] V.I. Veksler, J. of Phys. USSR **9**(1945)153

[13] A.H. Ho, R.H. Pantell and J. Feinstein, IEEE J. Quantum Electron. **QE-23**(1987)1545

[14] A.H. Ho, R.H. Pantell and J. Feinstein, Nucl. Instrum. and Methods **A318**(1991)758

[15] H. Leboutet, Proceedings of the 1991 IEEE Particle Accelerator Conference (May 6 – 9, 1991, San Francisco, USA), Vol.5, p.2763

[16] E.L. Saldin, E.A. Schneidmiller and M.V. Yurkov, "High efficiency FEL oscillator with time-dependent undulator tapering", Physics Letters A, in press

[17] E.L. Saldin, E.A. Schneidmiller and M.V. Yurkov, Nucl. Instrum. and Methods **A313**(1992)555

[18] E.L. Saldin, E.A. Schneidmiller and M.V. Yurkov, Sov. J. Particles & Nuclei **23**(1992)104

[19] K. Halbach, J. de Phys. **C1**, **44**(1983)211

[20] A.H. Ho, R.H. Pantell and J. Feinstein, Nucl. Instrum. and Methods **A296**(1990)631

[21] L.J. Milosevic et al., Trans. I.R.E. Vol. MTT-6 (1958)136

[22] Wang Yuan-ling, IEEE Trans. on Nucl. Sci. **NS-28**(1981)3526, IEEE Trans. on Nucl. Sci. **NS-30**(1983)3024

[23] M.I. Skolnik, Radar Handbook. McGraw-Hill Book Company, 1970

[24] J.R. Delayen et al., IEEE Trans. MAG. **MAG11**(1975)408

[25] W. Schnell, The CERN Study of a Linear Collider in the TeV Range, CERN SL/91-49, 1991

Received by Publishing Department
on November 4, 1993.

Салдин Е.Л., Шнейдмиллер Е.А., Юрков М.В. E9-93-401
Использование зависящего от времени радиочастотного поля для повышения КПД ЛСЭ-генератора

Работа посвящена изучению возможности и повышения КПД ЛСЭ-генераторов путем введения в область взаимодействия ускоряющего (или замедляющего) радиочастотного поля, зависящего от времени. Все предложенные схемы повышения эффективности базируются на существующем уровне технологии изготовления ВЧ-структур и ондуляторов. Реалистичность схем иллюстрируется результатами численного моделирования. Показано, что предлагаемый подход позволяет создавать ЛСЭ-генераторы инфракрасного и видимого диапазонов с КПД порядка 20%.

Работа выполнена в Лаборатории сверхвысоких энергий ОИЯИ.

Препринт Объединенного института ядерных исследований. Дубна, 1993

Saldin E.L., Schneidmiller E.A., Yurkov M.V. E9-93-401
High-Efficiency FEL Oscillator with Time-Dependent Microwave Field in Interaction Region

Various schemes of a high-efficiency FEL oscillator with the time-dependent accelerating (or decelerating) microwave field in the interaction region are proposed. All the schemes are based on standard accelerating structure and undulator technology. Feasibility of the proposed schemes is confirmed by results of numerical simulations. Realistic examples of FEL oscillators of infrared and visible wavelength ranges with an efficiency of about 20% are presented.

The investigation has been performed at the Laboratory of Particle Physics, JINR.

Preprint of the Joint Institute for Nuclear Research. Dubna, 1993